Hindawi
Advances in Materials Science and Engineering
Volume 2021, Article ID 6678802, 8 pages
https://doi.org/10.1155/2021/6678802

Research Article

Axial Performance of Steel Fiber-Reinforced Rubberized Concrete-Filled Circular Tubular Columns

Yu Deng,[1] Jiong-Feng Liang,[2] and Wei Li[3]

[1]*College of Civil and Architecture Engineering, Guangxi University of Science and Technology, Liuzhou, China*
[2]*Faculty of Civil&Architecture Engineering, East China University of Technology, Nanchang, China*
[3]*College of Civil Engineering and Architecture, Wenzhou University, Wenzhou, Zhejiang, China*

Correspondence should be addressed to Wei Li; liw1981@126.com

Received 17 October 2020; Revised 22 January 2021; Accepted 16 February 2021; Published 23 February 2021

Academic Editor: Hongtao Zhu

In order to study the axial performance of steel fiber-reinforced rubberized concrete-filled circular steel tubular columns, a total of 11 steel fiber-reinforced rubberized concrete-filled circular tubular columns are subjected to axial compression tests, considering the main parameters are rubber substitution rate, rubber particle size, steel fiber content, and concrete strength. The test results show that the use of rubber will reduce the bearing capacity of the columns but can increase the ductility of the columns. The smaller the rubber particles, the greater the reduction in the bearing capacity. The incorporation of steel fibers can increase the compressive strength of concrete, thereby improving the axial performance of the columns. The strength of concrete has the greatest influence on the columns, and the bearing capacity increases approximately linearly with the increase of concrete strength.

1. Introduction

Nowadays, how to dispose of waste rubber is a big problem. Waste rubber is a kind of solid waste. If it is directly buried and piled without treatment, it will cause great pollution to the environment [1–3]. Waste rubber mainly comes from waste tires. The world produces 1.5 billion waste tires each year, or more than 50 million tons. China is one of the countries with the largest output of waste tires. The output reached 300 million pieces, exceeding 10 million tons. This is the statistical data several years ago, and the data is still growing rapidly. It is expected that China's waste rubber output will exceed 20 million tons in 2020.

In today's resource-saving and environment-friendly society, research on the treatment methods of waste rubber plays a vital role in environmental protection. Regarding the utilization of waste rubber, two methods are mainly adopted: the first is the direct utilization method, and the second is the secondary utilization method. The direct utilization method includes using waste tires as buffer materials for docks and race tracks and burning treatment to collect heat energy. The secondary utilization method includes desulfurization to make recycled rubber, and processing into usable rubber powder. Because the output of waste rubber is too large, the direct utilization method used as a buffer material cannot completely consume waste rubber, and combustion treatment and desulfurization will generate a large amount of waste gas, so the waste rubber is processed into usable rubber powder.

Therefore, the combined use of rubber powder and concrete opens up a new method of recycling waste rubber. Mhaya et al. [4] studied the effect of different amounts of tire rubber scraps on the performance of newly designed concrete. The conclusion was as follows: the addition of rubber scraps would reduce the compressive, tensile, flexural strength and workability of concrete. But compared with traditional concrete, the newly designed hybrid material was relatively more economical, energy-saving, durable, acid-resistant, and environmentally friendly. Bisht and Ramana [5] evaluated compressive strength, flexural strength, density, and durability properties for the different proportions (0%, 4%, 4.5%, 5%, and 5.5%) of crumb rubber in concrete.

In view of other researches [1, 3, 6–11], it is found that rubber powder is added as an admixture to concrete, which will reduce the mechanical performance of concrete. Therefore, in order to make up the insufficient performance of rubber concrete, it is considered to add steel fibers to the rubber concrete, and the steel fibers are evenly distributed in the concrete to enhance the bonding performance of the concrete materials. Eisa et al. [12] studied the effect of the combination of rubber crumbs and steel fibers on the static load performance of reinforced concrete beams. The test results showed that the reinforced concrete beams could still maintain good performance when the amount of fine aggregate replaced by rubber crumbs was between 5% and 10%. At the same time, when the replacement rate of rubber crumbs was 10%, the specimen could have improved mechanical performance and toughness. Zhao et al. [13] studied the influence of steel fiber content, rubber content, and water-binder ratio on the shear properties of steel fiber rubber concrete. The results showed that the bridging effect of steel fiber and its synergy with rubber particles could significantly improve the shear resistance of concrete. The shear strength, peak deformation, and shear toughness of the specimens were significantly improved compared with the ordinary concrete and rubber concrete specimens. Xue et al. [14], Gul and Naseer [15], and Abdel and Hassan [16] found that the addition of steel fiber could not only compensate for the damage of rubber to concrete, but also ensure its good performance, respectively.

Filling steel fiber-reinforced rubberized concrete in steel tube can further restrain the deformation of concrete and increase its bearing capacity. Therefore, this study explores the axial performance of steel fiber-reinforced rubberized concrete-filled steel tube, to develop its feasibility for use in structural engineering.

2. Experimental Programme

2.1. Specimen Design. Considering the impact of rubber on the performance of concrete, a total of three types of rubber particle (RP) replacement rates, including 0%, 5%, and 10%, were designed to replace sand in concrete. In order to further study the role of rubber in rubber concrete, while considering the replacement rate of rubber particles, the influence of rubber powder of different diameters is also considered. This study considers rubber powder with three particle sizes of 20 mesh, 40 mesh, and 80 mesh. The size corresponding to 20 mesh is 0.825 mm, the size corresponding to 40 mesh is 0.475 mm, and the size corresponding to 80 mesh is 0.18 mm. For the influence of steel fiber (SF) content, four dosages of 0%, 0.6%, 0.9%, and 1.2% are considered. And the concrete strength grades considered are C20 (20 MPa), C30 (30 MPa), and C40 (40 MPa), respectively. A total of 11 specimens are designed for testing. The cross-sectional form of the specimens is shown in Figure 1, and the design factors of the specimens are shown in Table 1.

2.2. Material Properties. The coarse aggregate used for the concrete in this test is crushed stone with a diameter of 5–20 mm, with good particle size distribution. The fine aggregate uses medium-sized river sand, which is partially replaced by rubber particles, and the cement uses ordinary silicate. The water-cement ratio in cement and concrete is 0.45. The rubber is made by crushing and grinding waste tires, and the rubber particles obtained are shown in Figure 2. The rubber particles are sieved separately to collect rubber of different particle sizes. The shear steel fiber is used, which is shown in Figure 3, and the quality of the steel fiber is calculated according to the mass percentage of the steel in the same volume. Table 2 shows the mixing amount of each material in the concrete. Three $150 \times 150 \times 50$ mm cubes are made to determine the compressive strength of the concrete cube. The obtained compressive strength is shown in Table 2, where f_{cu} represents the compressive strength of the concrete cube.

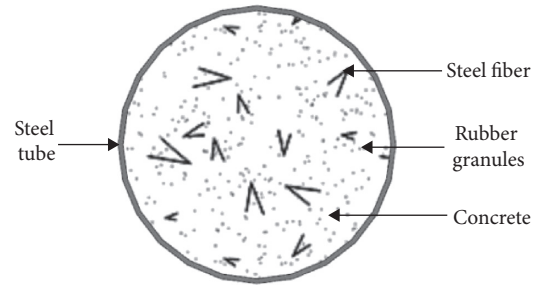

Figure 1: Section form of steel fiber-reinforced rubberized concrete-filled steel tube columns.

The steel tube used this time is a circular steel tube with a diameter of 114 mm, the wall thickness of the steel tube is 2 mm, and the length of the steel tube is 456 mm. The material properties of the obtained steel tubes are shown in Table 3, where f_y is the yield strength of the steel tube, f_u is the ultimate strength of the steel tube, and E_s is the elastic modulus of the steel tube.

2.3. Testing. The loading of the test specimen is carried out on a 300-ton electro-hydraulic servo pressure testing machine as shown in Figure 4. Two linear variable displacement transducers (LVDTs) were used to measure the axial deformation of the test specimen. During the test, the test phenomena are recorded and test photos are taken.

3. Results and Discussion

3.1. Failure Mode. In this test, the test phenomenon of each test specimen is roughly the same. Figure 5 shows the failure mode of the specimen under different rubber replacement rates. Figures 5(a)–5(c) show the specimens with rubber particle substitution rate of 0%, 5%, and 10%, respectively. It can be seen from Figure 5 that when the specimen is broken, the external steel tube is mainly buckled, and the upper and lower parts of the specimen are convex due to the existence of concrete, resulting in expansion. Comparing the deformation of the three specimens, it can be seen that the rubber particles are used to replace the fine aggregate, the deformation of the entire specimen in the axial direction is greater, and the buckling of the steel tube is more obvious.

Table 1: Design of various factors of the test specimen.

Specimen number	RP (%)	Rubber particle size	SF (%)	Concrete strength grade
SFRP-1	0	—	0.9	C30
SFRP-2	5	80 mesh	0.9	C30
SFRP-3	10	80 mesh	0.9	C30
SFRP-4	10	80 mesh	0.6	C30
SFRP-5	10	80 mesh	1.2	C30
SFRP-6	10	80 mesh	0.9	C20
SFRP-7	10	80 mesh	0.9	C40
SFRP-8	0	—	0	C30
SFRP-9	10	80 mesh	0	C30
SFRP-10	10	20 mesh	0.9	C30
SFRP-11	10	40 mesh	0.9	C30

Figure 2: Rubber particle.

Figure 3: Steel fiber.

Figure 6 shows the deformation characteristics of the tested specimens with different concrete strength. It can be found that the increase of concrete strength has a good restraint on the overall deformation of the specimen. Not only is the bending of steel tube reduced, but also the bending degree of the whole specimen is obviously reduced.

Figure 7 shows the failure mode of the specimen with 20-mesh rubber particles instead of fine aggregate. Compared to the specimen SFRP-3 with 80-mesh rubber particles, the failure modes of the specimen with 20-mesh rubber particles are very similar. Both of them have obvious convexity in the upper end area. At the same time, the middle steel tube of the specimen buckles, and the lower end of the specimen does not change significantly. The deformation degree of the specimen with 20-mesh rubber particles is smaller than that of the specimen with 80-mesh rubber particles.

3.2. Load-Displacement Relationship. Figure 8 shows the load-displacement curves of specimens with different rubber particle replacement rates.

It can be seen that as the replacement rate of rubber particles increases, the bearing capacity of the specimen decreases. Not only that, the addition of rubber particles will make the yield stage of the load-displacement curve of the specimen move back. It shows that adding rubber to concrete can enhance the deformability of the short column. It can be seen from Figure 8(a), with the increase of the rubber substitution rate, the degree of reduction in the bearing capacity of the specimen is not linear. When the rubber particle replacement rate increases by 5%, the bearing capacity of the specimen decreases by 9.0%, and when the rubber replacement rate continues to increase, the bearing capacity of the short column decreases more and more slowly. The 10% rubber particle replacement rate reduces the bearing capacity of the short column by about 15%.

The steel fiber can be evenly distributed in the concrete and bear the bridging function between the concrete bodies. Figure 9 shows the load-displacement curve of specimen with different steel fiber contents. It can be seen that the addition of steel fibers can increase the compressive strength of concrete, thereby directly increasing the bearing capacity of short columns. The addition of steel fiber will increase the displacement in the elastic phase of the load-displacement curve of the specimen.

According to the load-displacement curves of specimen with different rubber particle size shown in Figure 10, it can be found that the rubber particle size has little effect on the bearing capacity of the specimen and has a greater impact on

Table 2: Mixing amount of concrete.

Specimen number	RP (kg·m^{-3})	SF (kg·m^{-3})	Crushed stone (kg·m^{-3})	Sand (kg·m^{-3})	Cement (kg·m^{-3})	Water (kg·m^{-3})	f_{cu} (MPa)
SFRP-1	0	70.7	1257	531.0	422	190	35.3
SFRP-2	26.6	70.7	1257	504.4	422	190	29.8
SFRP-3	53.1	70.7	1257	477.9	422	190	27.1
SFRP-4	53.1	47.1	1257	477.9	422	190	24.5
SFRP-5	53.1	94.2	1257	477.9	422	190	29.2
SFRP-6	53.1	70.7	1257	477.9	422	190	22.3
SFRP-7	53.1	70.7	1257	477.9	422	190	40.6
SFRP-8	0	0%	1257	531.0	422	190	32.3
SFRP-9	53.1	0%	1257	477.9	422	190	23.1
SFRP-10	53.1 (20)	70.7	1257	477.9	422	190	28.2
SFRP-11	53.1 (40)	70.7	1257	477.9	422	190	27.6

Table 3: Material performance of steel tube.

Type	f_y (MPa)	f_u (MPa)	E_s(GPa)
Steel tube	382.3	441.2	202.1

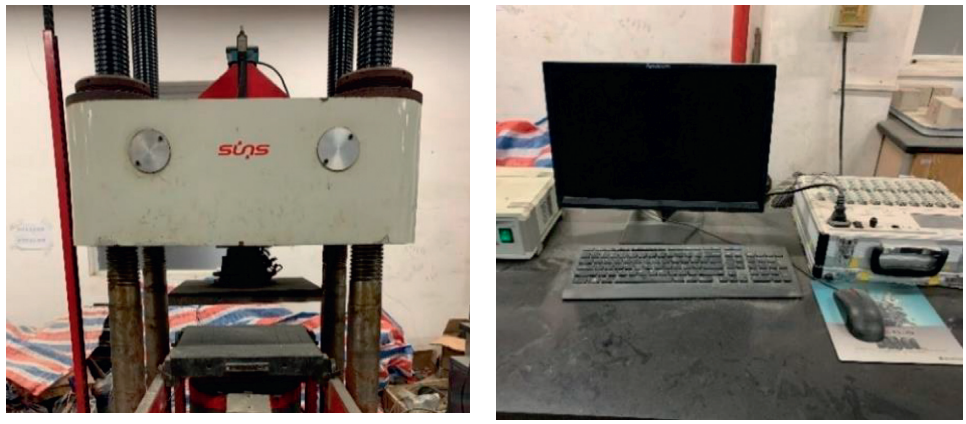

(a) (b)

Figure 4: Electro-hydraulic servo pressure testing machine. (a) Pressure testing machine. (b) Data collection system.

(a) (b) (c)

Figure 5: Failure mode of specimens with different rubber particle replacement rates. (a) SFRP-1. (b) SFRP-2. (c) SFRP-3.

(a) (b)

Figure 6: Failure mode of specimens with different concrete strengths. (a) SFRP-6. (b) SFRP-7.

Figure 7: Damage of large particle rubber specimen.

the deformation of the specimen. With the increase of the rubber particle size, the bridging effect between the concrete and the steel fiber in the steel tube is strengthened, but this improvement is not very obvious.

Concrete strength is the biggest factor that affects the ultimate bearing capacity of short columns. With the increase of concrete strength, the compressive strength of steel fiber-reinforced rubberized concrete will be significantly improved. Figure 11 describes the load-displacement curve of specimens with different concrete strength. It can be clearly seen from Figure 11 that when the design concrete strength grade is C40, the bearing capacity of the steel fiber-reinforced rubberized concrete-filled steel tube short column is significantly improved, and the increase rate reaches

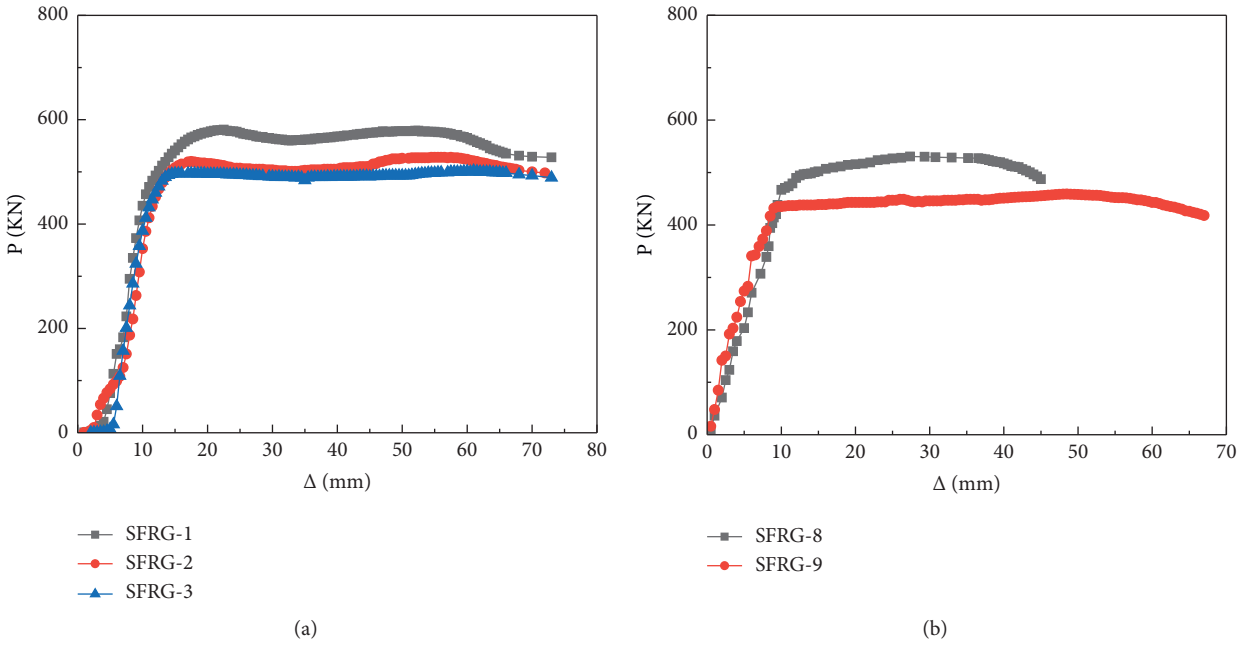

Figure 8: Load-displacement curves of specimens with different rubber particle replacement rates. (a) 0.9% SF and (b) 0% SF.

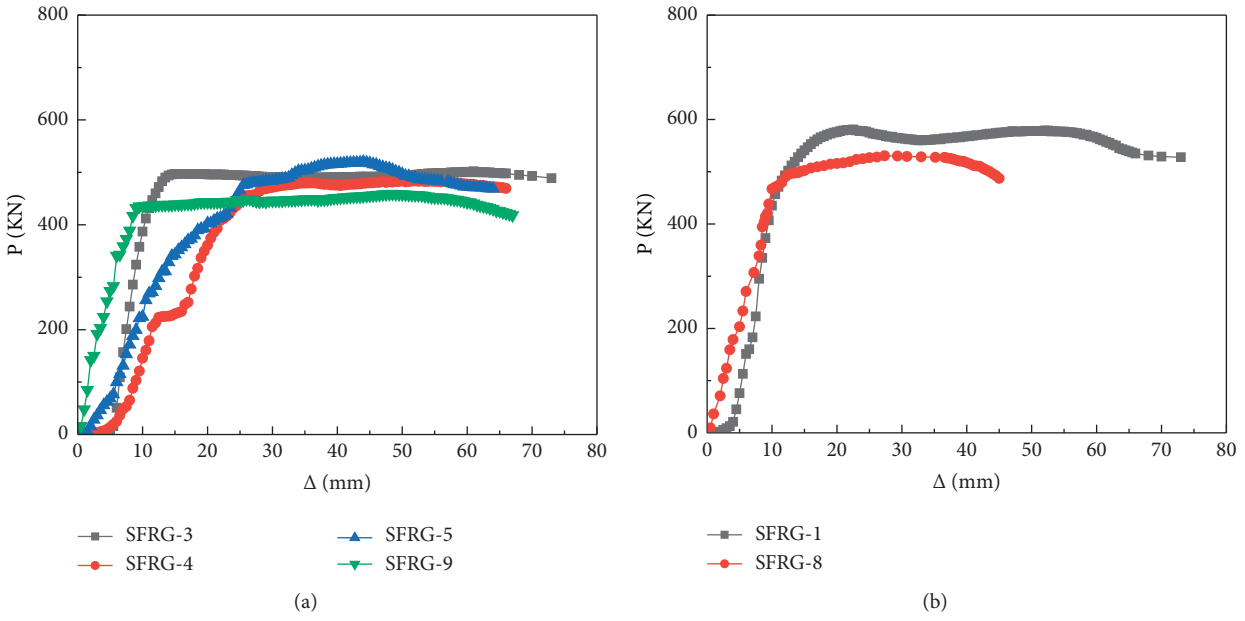

Figure 9: Load-displacement curve of specimen with different steel fiber contents. (a) 10% RP and (b) 0% RP.

25.8%. As the concrete strength increases, the ultimate displacement of the specimen is significantly reduced, which corresponds to the failure phenomenon in Figure 6(b).

3.3. Ductility. The displacement ductility coefficient is used to describe the ductility and deformability of steel fiber-reinforced rubberized concrete-filled steel tube short columns. The displacement ductility coefficient is defined as the ratio of the ultimate displacement to the yield displacement. The ultimate displacement is expressed by the displacement corresponding to the ultimate load in the load-displacement curve, and the yield displacement is expressed by the displacement of the point where the slope reaches the maximum in the load-displacement curve. The displacement ductility coefficient is obtained by equation (1), where μ is the displacement ductility coefficient, Δ_m is the ultimate displacement, and Δ_y is the yield displacement:

$$\mu = \frac{\Delta_m}{\Delta_y}. \tag{1}$$

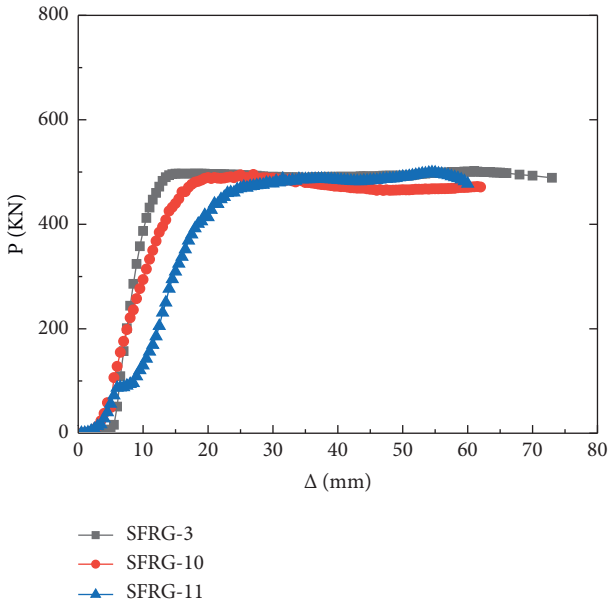

Figure 10: Load-displacement curve of specimen with different rubber particle size.

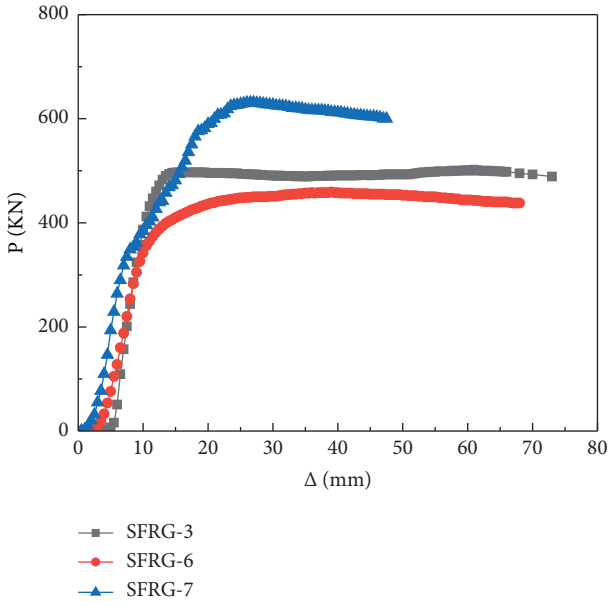

Figure 11: Load-displacement curve of specimen with different concrete strength.

According to the results in Table 4, the addition of rubber particles and steel fibers has little effect on the yield displacement of the specimen, but it can significantly increase the ultimate displacement of the specimen and increases its ductility coefficient. The smaller the particle size of the rubber particles, the greater the ductility coefficient of the specimen. The single incorporation of steel fiber will reduce the ductility coefficient of the specimen, but its combination with rubber particles can improve the ductility as a whole, and the increase in concrete strength will also reduce the ductility coefficient of the specimen. In general, using rubber instead of sand and adding a certain amount of steel fiber in concrete can improve the ductility of the specimen.

Table 4: Calculation of displacement ductility coefficient.

Specimen number	Δ_y (mm)	Δ_m (mm)	μ
SFRP-1	10.5	22.5	2.14
SFRP-2	11.5	55.5	4.83
SFRP-3	11.0	61.0	5.55
SFRP-4	22.0	50.0	2.27
SFRP-5	11.0	44.0	4.00
SFRP-6	9.5	39.0	4.11
SFRP-7	7.0	27.0	3.86
SFRP-8	10.0	27.3	2.73
SFRP-9	6.0	26.0	4.33
SFRP-10	12.5	27.0	2.16
SFRP-11	18.0	54.5	3.03

Table 5: Stiffness calculation.

Specimen number	P_y (KN)	ε_y	K_{ss} (KN)	RS
SFRP-1	457.0	0.0230	19846.86	0.93
SFRP-2	434.0	0.0252	17209.04	0.81
SFRP-3	432.0	0.0241	17908.36	0.84
SFRP-4	408.4	0.0482	8465.018	0.40
SFRP-5	269.1	0.0241	11155.42	0.52
SFRP-6	326.0	0.0208	15648.00	0.73
SFRP-7	318.0	0.0154	20715.43	0.97
SFRP-8	467.1	0.0219	21299.31	1.00
SFRP-9	341.0	0.0132	25916.00	1.22
SFRP-10	384.7	0.0274	14033.86	0.66
SFRP-11	392.2	0.0395	9935.73	0.47

3.4. Stiffness. The stiffness is defined by the secant stiffness in the elastic stage before the specimen yields. The secant stiffness is calculated according to formula (2), where K_{ss} is the secant stiffness, P_y is the yield load, and ε_y is the strain corresponding to the yield load. In order to facilitate the description of the change of the stiffness of the short columns, the stiffness of the specimen without steel fiber and rubber is defined as 1, and the relative stiffness (RS) is obtained.

$$K_{ss} = \frac{P_y}{\varepsilon_y}. \tag{2}$$

From the data in Table 5, it can be seen that the stiffness of steel fiber-reinforced rubberized concrete-filled steel tube short columns will decrease compared with ordinary concrete-filled steel tube short columns. Among them, the specimens with 0.6% steel fiber content and the specimens with a rubber particle size of 40 mesh have the largest decrease in stiffness, exceeding 50%. The average stiffness of other specimens with steel fiber and rubber reduces 20%. On the whole, the degree of stiffness reduction is within an acceptable range.

4. Conclusions

Through the above experimental research and data analysis, we can get the following conclusions:

(i) The damage of the steel fiber-reinforced rubber concrete-filled steel tube short column is mainly caused by the buckling of the steel tube and the expansion of the concrete.

(ii) The replacement of rubber particles will reduce the bearing capacity of the test specimen, and with the increase of the rubber substitution rate, the bearing capacity of the test specimen will decrease; the addition of rubber particles can also improve the ductility of the test specimen; the rubber particle with the larger particle size is more beneficial to the performance of the specimen.

(iii) The addition of steel fibers can compensate for the reduction in bearing capacity caused by rubber particles, and the addition of steel fibers can inhibit the transverse expansion of the concrete during the axial compression process.

(iv) The strength of concrete has the greatest influence on the bearing capacity of the specimen. As the strength of concrete increases, the bearing capacity of the specimen increases significantly, but the increase of the concrete strength will reduce the ductility of the specimen.

(v) The stiffness of steel fiber-reinforced rubber concrete-filled steel tube short column is lower than that of ordinary concrete-filled steel tube.

In order to better study the axial compression performance of steel fiber-reinforced rubberized concrete-filled circular tubular columns, the finite element analysis (FEA) will be further studied in the future.

Data Availability

The data used to support the findings of this study are included within the article.

Conflicts of Interest

The authors declare that they have no conflicts of interest regarding the publication of this paper.

Acknowledgments

This work was supported by the Chinese National Natural Science Foundation (Nos. 51868001 and 52068001), the Project of Academic and Technological Leaders of Major Disciplines in Jiangxi Province (No. 20204BCJL2037), the Natural Science Foundation of Jiangxi Province (No. 20202ACBL214017), and the Hundred People Voyage Project of Jiangxi Province, which are gratefully acknowledged.

References

[1] F. Aslani, G. Ma, D. L. Yim Wan, and G. Muselin, "Development of high-performance self-compacting concrete using waste recycled concrete aggregates and rubber granules," *Journal of Cleaner Production*, vol. 182, pp. 553–566, 2018.

[2] Q. H. Han, G. Yang, J. Xu, and Y. H. Wang, "Fatigue analysis of crumble rubber concrete-steel composite beams based on XFEM," *Steel & Composite Structures*, vol. 25, no. 1, pp. 257–284, 2017.

[3] R. B. Murugan and C. Natarajan, "Investigation on the use of waste tyre crumb rubber in concrete paving blocks," *Computers and Concrete*, vol. 20, no. 3, pp. 311–318, 2017.

[4] A. M. Mhaya, G. F. Huseien, A. R. Z. Abidin, and M. Ismail, "Long-term mechanical and durable properties of waste tires rubber crumbs replaced GBFS modified concretes," *Construction and Building Materials*, vol. 256, 2020.

[5] K. Bisht and P. V. Ramana, "Evaluation of mechanical and durability properties of crumb rubber concrete," *Construction and Building Materials*, vol. 155, pp. 811–817, 2017.

[6] K. C. Williams and P. Partheeban, "An experimental and numerical approach in strength prediction of reclaimed rubber concrete," *Advances in Concrete Construction*, vol. 6, no. 1, pp. 87–102, 2018.

[7] M. Emiroglu, S. Yildiz, and M. H. Kelestemur, "A study on dynamic modulus of self-consolidating rubberized concrete," *Computers and Concrete*, vol. 15, no. 5, pp. 795–805, 2015.

[8] W. Feng, F. Liu, F. Yang, L. Li, and L. Jing, "Experimental study on dynamic split tensile properties of rubber concrete," *Construction and Building Materials*, vol. 165, pp. 675–687, 2018.

[9] S. Guo, Q. Dai, R. Si, X. Sun, and C. Lu, "Evaluation of properties and performance of rubber-modified concrete for recycling of waste scrap tire," *Journal of Cleaner Production*, vol. 148, pp. 681–689, 2017.

[10] M. K. Ismail and A. A. Hassan, "A Performance of full-scale self-consolidating rubberized concrete beams in flexure," *ACI Materials Journal*, vol. 113, no. 2, pp. 207–218, 2016.

[11] S. Padhi and K. C. Panda, "Fresh and hardened properties of rubberized concrete using fine rubber and silpozz," *Advances in Concrete Construction*, vol. 4, no. 1, pp. 49–69, 2016.

[12] A. S. Eisa, M. T. Elshazli, and M. T. Nawar, "Experimental investigation on the effect of using crumb rubber and steel fibers on the structural behavior of reinforced concrete beams," *Construction and Building Materials*, vol. 252, 2020.

[13] Q. H. Zhao, S. Dong, and H. Zhu, "Experimental study on shear behavior of steel fiber-rubber/concrete," *Acta Materiae Compositae Sinica*, vol. 122020, in Chinese.

[14] G. Xue, S. Hou, and J. G. Niu, "Experimental research on pavement performance of rubber concrete incorporated with plastic-steel fiber," *Building Structures*, vol. 49, no. 12, pp. 98–108, 2019, in Chinese.

[15] S. Gul and S. Naseer, "Concrete containing recycled rubber steel fiber," *Procedia Structural Integrity*, vol. 18, 2019.

[16] A. B. H. Abdel and A. A. A. Hassan, "Effect of combining steel fibers with crumb rubber on enhancing the behavior of beam-column joints under cyclic loading," *Engineering Structures*, vol. 182, 2019.